INVESTIGATION OF FLOW BOILING HEAT TRANSFER CHARACTERISTIC OF MIXTURE REFRIGERANT L-41B IN A HORIZONTAL SMOOTH TUBE

Jinyou-Qiu[a,b,c*1], Yonglin-Fang[a], Guilong-Dai[a], Xiaoming-Chen[a],
Hua-Zhang[b], Weidong-Wu[b] Zhihon-Wu[c]

[a]Key Laboratory of New Energy and Energy-saving in Building, Fujian University of Technology, Fuzhou 350118, China

[b]School of Energy and Power Engineering, University of Shanghai for Science and Technology, Shanghai 200093, China

[c]CSCEC Strait Construction and Development Co., Ltd, Fuzhou, 350015, China

Abstract：The saturated flow boiling heat transfer characteristics of L-41b (R1234ze(E)/R32 (27/73 mass %)) inside an 8 mm ID horizontal tube were investigated. The experiment were carried out at the saturation temperature of 10 to 20 °C with heat flux ranging from 5 to 10 kW·m^{-2} and mass flux ranging from 200 to 500 kg·m^{-2}·s^{-1}. The influence of mass flux, heat flux and quality on the heat transfer coefficients were examined and discussed. The experimental data of local heat transfer coefficients were compared with four well-known correlations available in literatures. Additionally, a new vapor-phase multiplier correlation to predict the local heat transfer coefficients of L-41b flow boiling inside smooth tubes was developed. The results show that the deviations of the new correlation are within -24.98% to +14.68% to the experimental data and that the 95% prediction values are within ±15%.

Keywords：R1234ze(E); L-41b; Flow Boiling Heat Transfer; Correlation

1. Introduction

As refrigerants, Hydrofluorocarbons (HFCs) are widely used in refrigeration and heat pump system. Although HFCs are non-ozone depleting, they do have large global warming potential (GWP), which could lead to global warming[1-2]. Looking for the proper low GWP alternative refrigerant is important and urgent for the refrigeration and air conditioning.

Recently, many alternative refrigerants were proposed, including low GWP HFCs, natural refrigerants, and hydrofluoroolefins (HFOs). Howerer, these efforts still have not achieved satisfactory success, because rare pure refrigerants can completely meet the environmental, thermodynamic, and safety requirements of new-generation refrigerants [3].

In the recent years, HFOs (Hydro-Fluoro-Olefines) have attracted great attention because of the low GWP value. In particular, R1234ze(E) as a kind of HFOs which was found to be low flammability, non-toxicity, zero ozone depletion potential (ODP) and quite low global warming potential (GWP<1)[4]. R1234ze(E) was supposed to be the most promising refrigerant candidate in heat pump system[5,6]. In fact, R32 has gained much attention due to its high latent heat, zero ODP, and middle GWP, especially in the field of ASHPs, and it is expected to replace R410A[7]. However, its high discharge temperature and slight flammability limit its applications in other fields. In order to cover more wide range of air-conditioner, heat pump, and refrigeration systems, refrigerant mixtures R32/R1234ze(E) have attracted great attention in the field of air conditioning and heat pumps due to their excellent properties[8]. Tab. 1 lists the refrigerants named by the ASHRAE Standard(34–2013)

Corresponding Author's E-mail: junior51020@163.com

as well as unnamed but widely studied refrigerant mixtures that mainly contain R32 and R1234ze(E)[9]. The zeotropic mixture of R1234ze(E) and R32 with mass fraction of 27/73 which was named L-41b was suggested to be an substitute of R410A in a recent study by AHRI (The Air-Conditioning, Heating, and Refrigeration Institute) [10].

Most of the studies available in literatures on the mixture of R1234ze(E) and R32 focused on the thermodynamic properties (Akasaka R, 2013[11]; Cui J. et al., 2016[12]; Jia T. et al., 2016[13]) and drop-in replacements in existing refrigeration system (Cheng Z. et al.,2017[14]; Lee H. et al., 2016[15]; Francisco M. et al., 2014[16]; Adrian M. B., et al., 2014[17,18]). Sungjin In et al.[19] presented L41b drop-in test data of an R410a residential heat pump system. It was found that the drop-in capacities of L41b systems were 89–94% of those of R410A systems, while that of the COPs of L41b systems were 104–105% of those in R410A systems.

However, flow boiling heat transfer characteristics of the mixture of R1234ze(E) and R32 are rarely reported. Hossaind et al.[20] investigated the flow boiling heat transfer characteristics of R1234ze(E) and the mixture of R1234ze(E)/R32 with mass fraction of 55/45 in horizontal tube with inner diameter of 4.35 mm. It is indicated that the local heat transfer coefficients of R1234ze(E)/R32 (mass ratio: 55/45) are slight lower than those of pure R1234ze(E) due to the inferior liquid thermal conductivity and the effect of mass transfer resistance of the mixture.

In this work, we experimentally investigated the local heat transfer coefficients during saturation flow boiling of the mixture L-41b in horizontal tube with an inner diameter of 8 mm. The experimental results were obtained at the saturation temperature of 10 to 20 ^{o}C, heat flux ranging from 5 to 10 kW· m^{-2}, mass flux ranging from 200 to 500 kg· m^{-2}· s^{-1}. Moreover the experimental heat transfer coefficients are compared with the predicted results obtained by using some empirical prediction models from the literatures (Tab.4[21-25]). Additionally, a new vapor-phase multiplier correlation to predict the local heat transfer coefficients of L-41b flow boiling inside smooth tubes is developed based on the model of Choi et al.

Tab.1. List of low GWP refrigerant candidates in Phase I (R410A candidates)

Baseline	Refrigerant	Composition	(Mass%)	Classification	GWP_{100}
R410A	L41a	R32/R1234yf/R1234ze(E)	（73/15/12）	A2L	494
	L41b	R32/ R1234ze(E)	（73/27）	A2L	494
	R32/R134a	R32/ R134a	（95/5）	A2L	713
	R32/R152a	R32/ R152a	（95/5）	A2L	647

2. Experimental setup

Fig.1 shows the schematic of experimental apparatus in this study. The test fluid is driven by magnetic gear pump and its flow rate is measured by Coriolis effect mass flow meter. The fluid flow rate can be adjusted by the electric motor speed by an inverter or bypass-valve installed between inlet and outlet of the gear pump. The refrigerant in the main loop passes through sub-cooler to offset the enthalpy increasing in pump, and to ensure the refrigerant being in sub-cooled condition when it passes through the mass flow meter.

In front of the test section, a preheater is used to adjust the inlet vapor quality of the test fluid. The heating capacity of the preheater can be adjust by the voltage supply. After that, the refrigerant passes through the test section and condenser, sequentially. Along the test loop, two sight glasses are installed at the inlet and outlet of the test section, allowing to see the two-phase flows. The condenser is installed in a thermostatic bath which consists of a refrigeration system, a heating system and a stirrer. The temperature of thermostatic bath can be adjusted in the range between -20 °C and 30 °C. The test fluid goes back to the liquid reservoir after condensed in the thermostatic bath. The experimental setup was introduced in detail in the published paper[26].

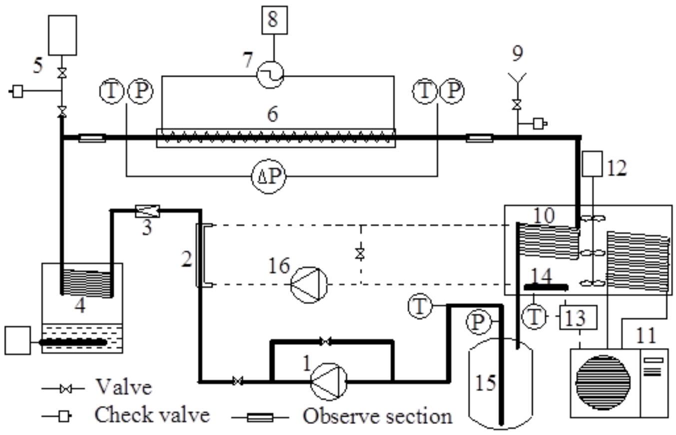

1-magnetic gear pump 2-sub-cooler 3-Coriolis mass flow meter 4-preheater 5-sampling port 6-test section 7-electric heater 8-electricity meter 9-charging port 10-condenser 11-refrigerating unit 12-stirrer 13-controller 14-heater 15-liquid reservoir 16-sub-cooler recycle pump

Fig.1. Schematic diagram of the experimental system

The schematic of the test section is shown on Fig.2. The test tube are made of copper with an inner diameter of 8 mm and a length of 2400 mm. Along the axial of the test tube, five temperature measuring point are evenly distributed. The wall temperature of each point is measured by the thermocouples embedded in the top, bottom, right and left of the exterior test tube wall. Two pressure transducers are used to measure the inlet and outlet pressures of the test section. The pressure drop between the inlet and the outlet of the test section is measured by a differential pressure transducer. The electric heating tape tightly adhered to the copper surface to generate heat flux as showed in Fig.3. The heat flux in the test section is varied by adjusting the input power of the electric heating tape. In order to reduce heat loss, the test section is insulated by glass wool, insulation cotton and trapping belt. The total heat losing from the test section is estimated to be less than 3.0%.

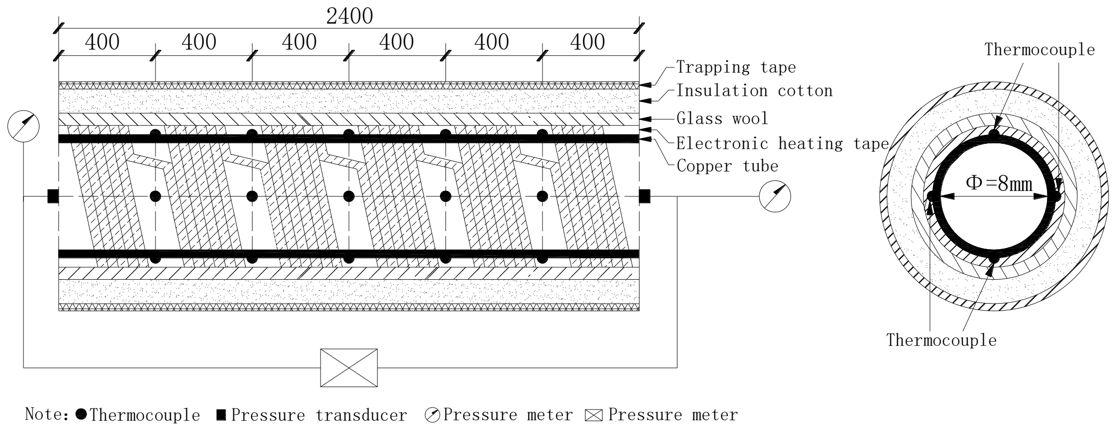

Fig.2. Schematic diagram of the test section

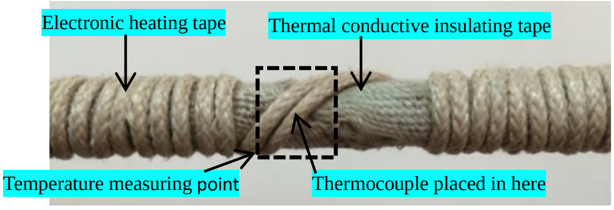

Fig.3. Structure of temperature measuring point in the test section

3. Data reduction and uncertainty analysis

3.1 Data reduction

The local saturation flow boiling heat transfer coefficient is calculated by the following equation:

$$h_{tp} = q/(T_{wi} - T_{sat}) \tag{1}$$

$$q = Q_{test}/(\pi d_{in} \Delta z) \tag{2}$$

where, q represents the inner wall heat flux of the tube. Q_{test} is the total heat amount in the test section which can be obtained by measuring the total heat input and the heat losses. T_{sat} is the saturation temperature of the fluid, which is determined by the measuring the pressure at the inlet of the test section and the pressure drop along the test section. T_{wi} is the average inner wall temperature, which can be calculated by the following equation:

$$T_{wi} = \frac{1}{20}\sum_{i=1}^{20} T_{wo,i} - \ln\left(\frac{d_{wo}}{d_{wi}}\right)\frac{Q_{test}}{2\pi\lambda\Delta z} \tag{3}$$

The inlet vapor quality of the test section can be calculated from the energy balance in the test section and the preheater section, which is obtained from the following equations:

$$i_{\text{test,in}} = X_{\text{in}} i_{\text{test,v,in}} + (1 - X_{\text{in}}) i_{\text{test,l,in}} \tag{7}$$

$$i_{\text{test,out}} = X_{\text{out}} i_{\text{test,v,out}} + (1 - X_{\text{out}}) i_{\text{test,l,out}} \tag{8}$$

$$i_{\text{test,in}} = i_{\text{preh,in}} + \frac{Q_{\text{preh}}}{m} \tag{9}$$

$$i_{\text{test,out}} = i_{\text{preh,in}} + \frac{Q_{\text{preh}} + Q_{\text{test}}}{m} \tag{10}$$

where, i indicates the specific enthalpy, the subscript "in" and "out" indicate the inlet and outlet of the test section, the subscript "v" and "l" indicate the vapor and liquid. Q_{preh} represents the thermal power applied to the preheater. Q_{test} represents the thermal power applied to the test section. m is the flow rate of the test fluid. The average vapor quality is defined by Eq.(11).

$$X_{\text{ave}} = \frac{X_{\text{in}} + X_{\text{out}}}{2} \tag{11}$$

The thermodynamic parameters of pure substances are from REFPROP V9.0 (Lemmon et al., 2009). Tab.2 summarizes the thermodynamic parameters of the test fluids, which are obtained by using non-ideal mixing rule proposed by Kedzierski et al[27].

Tab.2. Thermodynamic parameters of L-41b

Parameters	Unit	T = 283 K	T = 293 K
Molecular weight	$g \cdot mol^{-1}$	68.8	68.8

GWP(100 year)	—	493	493
Liquid density	$kg \cdot m^{-3}$	1071.2	1034.7
Vapor density	$kg \cdot m^{-3}$	26.5	35.9
Liquid thermal conductivity	$mW \cdot mK^{-1}$	121.8	107.6
Specific heat	$kJ \cdot (kgK)^{-1}$	1.678	1.746
Surface tension	$mN \cdot m^{-1}$	9.67	8.11
Latent heat	$kJ \cdot kg^{-1}$	266	251

3. Uncertainty analysis

All the test parameters were recorded by a data acquisition system when the system reached the steady-state conditions. The temperatures and pressures of the test section were continuously monitored. The criterion for the steady-state conditions was that the variations of the wall and refrigerant saturation temperatures were less than ±0.1 K for 10 min. The fluid mass flux was measured by a Coriolis mass flow meter with an uncertainty of ±1% RS. The power of the preheater was measured by a wattmeter with an uncertainty of ±0.4%. The saturation fluid temperature was measured by the PT100 Ω resistance thermometer with an uncertainty of ±0.1 °C. The temperature of the out wall was measured by T-type thermocouples with an uncertainty of ±0.1℃. Tab.3 summarizes the measuring ranges and uncertainties of the measurement instruments. The uncertainty analysis was carried out by the method of Moffat[28]. The relative standard uncertainty of heat transfer coefficient can be expressed by the following equation:

$$\frac{u(h)}{h} = \sqrt{\left(\frac{u(q)}{q}\right)^2 + \left(\frac{u(T_{wi})}{T_{wi}-T_{sat}}\right)^2 + \left(\frac{u(T_{sat})}{T_{wi}-T_{sat}}\right)^2} \quad (12)$$

Where $u(q)$ is the combined standard uncertainty of heat flux, $u(T_{wi})$ is the combined standard uncertainty of the wall temperature, $u(T_{sat})$ is the combined standard uncertainty of the saturation temperature. Under the operation conditions, the experimental heat transfer coefficients obtained in this work present a minimum value and a maximum value of 2.3% and 12.4%, respectively.

Tab.3. Measurement instruments and their uncertainties

Parameters	Instrument	Range	Uncertainty
Refrig. temp.	PT100Ωthermometers	-50～200 °C	±0.1 °C
Wall temp.	T-type thermocouple	-20～100 °C	±0.1 °C
Pressure	Absolute pressure transducer	0～2MPa	±0.05%FS
Pressure drop	Differential pressure transducer	0～40kPa	±0.075%
Mass flux	Coriolis mass flow meter	0.1～5kg/min	±1%RS
Electricity	Power meter	5～500V；0.01～40A	±0.4%
Enthalpy	REFPROP V9.0	—	±0.02%

4. Results and discussion

In the experiment, flow boiling characteristics of L-41b have been investigated under different operation conditions as listed in Tab.4. Then the effects of different parameters on heat transfer coefficient were analysed.

Tab.4. Test conditions for the experiment

Mass flux ($kg\cdot m^{-2}\cdot s^{-1}$)	Heat flux ($kW\cdot m^{-2}$)	Quality	Saturation Temperature (^{o}C)
200	5.0；10.0	0.075～0.785	10±0.5；20±0.5
300	5.0；10.0	0.075～0.785	10±0.5；20±0.5
400	5.0；10.0	0.075～0.785	10±0.5；20±0.5
500	5.0；10.0	0.075～0.785	10±0.5；20±0.5

4.1 Experimental heat transfer coefficients

Fig.4 and Fig.5 show the local heat transfer coefficients of L-41b as a function of vapor quality obtained at saturation temperature of 10.0±0.5 ^{o}C and 20.0±0.5 ^{o}C with two heat fluxes (5.0 $kW\cdot m^{-2}$ and 10.0 $kW\cdot m^{-2}$) and several mass fluxes ranging from 200 to 500 $kg\cdot m^{-2}\cdot s^{-1}$, respectively. The local heat transfer coefficient of L-41b gradually increases and then decreases with increasing vapor quality.

The increase of the mass flux leads to a significant enhancement of heat transfer coefficients. This causes a strong increase of the mean fluid velocity during evaporation and a consequent enhancement of the convective boiling contribution. In particular, the ρ_v/ρ_l ratio are about 0.0247 and 0.0367 with the saturation temperature of 10 ^{o}C and 20 ^{o}C, respectively. This causes a strong increase of the mean fluid velocity during evaporation and a consequent enhancement of the convective boiling contribution. When the mass flux increases from 300 $kg\cdot m^{-2}\cdot s^{-1}$to 400 $kg\cdot m^{-2}\cdot s^{-1}$, the heat transfer coefficient increase by 9.7% at heat flux of 10.0 $kW\cdot m^{-2}$ and saturation temperature of 10 ℃. when the mass flux increases from 400 $kg\cdot m^{-2}\cdot s^{-1}$to 500 $kg\cdot m^{-2}\cdot s^{-1}$, the heat transfer coefficient increase by 8.5% at heat flux of 10.0 $kW\cdot m^{-2}$ and saturation temperature of 10 ℃.

The increase of the heat flux leads to a slight increase of the local heat transfer coefficients in the whole range of vapor quality. When the heat flux increases from 5 $kW\cdot m^{-2}$ to 10.0 $kW\cdot m^{-2}$, the heat transfer coefficient increase by 4.74% averagely. The heat flux has a stonger effect on the heat transfer coefficients in low vapor quality range than that in high vapor quality due to the dominant nucleate boiling in low vapor quality.

The increase of the saturation temperature leads to a slight descrease of the local heat transfer coefficients in the whole range of vapor quality. The saturation temperature has a stronger effect on the heat transfer coefficients in high vapor quality range than that in low vapor quality. When the saturation temperature increases from 10 ℃ to 20 ℃, the heat transfer coefficient increases by 7.52% averagely.

From literatures, it is well accepted that heat transfer coefficient of zeotropic binary mixture is less than the two pure substances because of the concentration gradients. Since the heat transfer degradation of zeotropic mixture L-41b is relatively weak, the heat transfer performance of L-41b is greater than that of R1234ze(E)/R32 (ratio: 55/45) obtained by Hossain M.A[20]. Because the heat transfer degradation of R1234ze(E)/R32 (ratio: 55/45) is stronger than that of L-41b due to the difference of temperature glide ($\Delta T_{R1234ze(E)/R32\ (ratio:\ 55/45)}$=8.9 ^{o}C, $\Delta T_{L\text{-}41b}$=3.1 ^{o}C). Moreover，the main composition of L-41b is R32 with great heat transfer performance as suggested by many researchers.

4.2 Predictability verification of exiting correlations to experimental data

In this paper, a comparison of experimental heat transfer coefficients of L-41b with the predicted results using the four empirical correlations is shown in Tab.4[21-25]. The absolute average deviation

(AAD) and root mean square deviation (RMS) of the correlations and the experimental data are summarized in Tab.5.

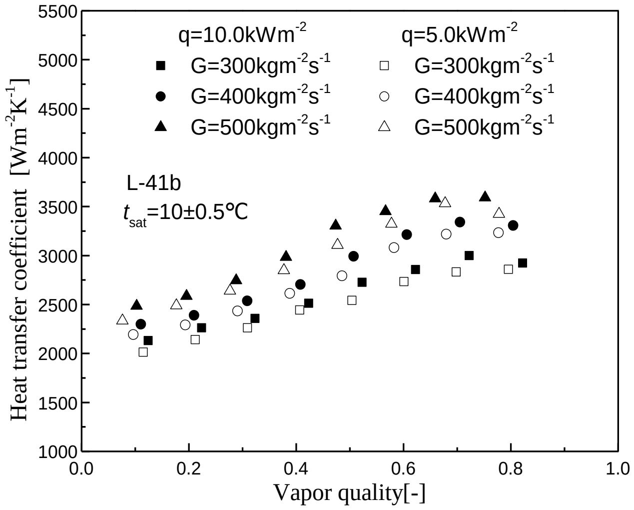

Fig.4. Heat transfer coefficients versus vapor quality (t_{sat} =10℃)

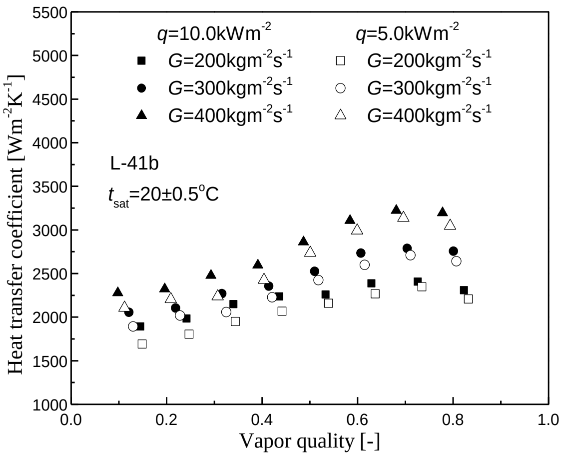

Fig.5. Heat transfer coefficients versus vapor quality (t_{sat} =20℃)

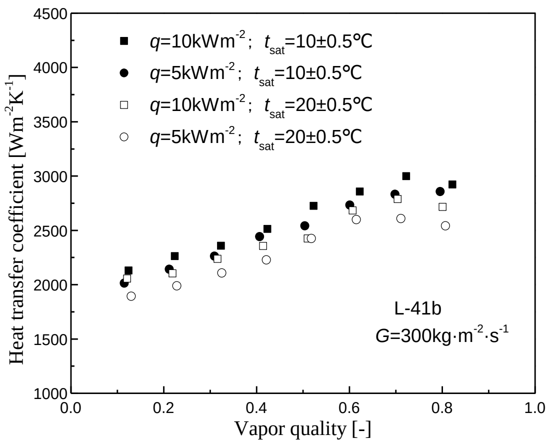

Fig.6. Heat transfer coefficients versus vapor quality at different saturation temperature

Among the results, the correlation of Choi achieves the best agreement with experimental data. The total absolute average deviation is 20.7%. Moreover, approximately 90% of experimental points are within an error bandwidth of ±30% of the prediction. Note that the total absolute average deviations obtained with Choi method and Sami method are 20.07% and 20.1%, respectively. Both are acceptable for engineering applications. The correlation (Bivens and Yokozeki; Liu and Winterton) underestimates the measured heat transfer coefficients.

Tab.4. Correlation of flow boiling heat transfer coefficient.

1.Bivens and Yokozeki[23](1994)

$h_{tp,m} = \left[{h_{nb}}^{2.5} + {h_{cv}}^{2.5}\right]^{1/2.5}$; $h_{cv} = Fh_l R$; $h_{nb} = 55Pr^{0.12}(-\log_{10} Pr)^{-0.55} M_w^{-0.5} q^{n0.67}$; $h_{tp,m} =$

$h_{tp}/\left(1 + h_{tp} T_{int} q\right)$; $T_{int} = 0.175\Delta t_{bp}[1 - exp(-q/1.3/10^4/\rho_l/\Delta h_v)]$;

$F = (0.29 + 1/X_{tt})^{0.85}$; $R = 2.15\ when\ Fr_l > 0.25$; $R = 2.83\ when\ Fr_l \leq 0.25$

2.Correlations of Choi et al. [24](2000)

$h_{tp,m} = Eh_{sp} + F_M Sh_{nb}$; $h_{cv} = 0.023(Re_l)^{0.8}(Pr_l)^{0.4}(\lambda_l/d)$; $E = 49.971Bo^{0.383}X_{tt}^{-0.758}$;

$h_{nb} = 207(\lambda_l/D_{bl})[qD_{bl}/(\lambda_l T_{sat})]^{0.674}(\rho_v/\rho_l)^{0.581} Pr_l^{0.533}$; $S = 0.909Co^{0.301}$;

$F_M = \left\{1 + 0.039\left[C_{p,l}\left(T_{dew} - T_{bp}\right)/H_{lv}\right]\right\}^{-1}$

3.Liu and Winterton(1991) [25]and Sun et al. [26](2007)

$h_{tp,m} = [(Eh_{cv})^2 + (F_M Sh_{nb})^2]^{0.5}$; $h_{cv} = 0.023(Re_l)^{0.8}(Pr_l)^{0.4}(\lambda_l/d)$;

$h_{nb} = 55Pr^{0.12}(-\log_{10} Pr)^{-0.55} M_w^{-0.5} q_{ch}^{n0.67}$; $E = [1 + xPr_l(\rho_l/\rho_v - 1)]^{0.35}$;

$S = \left(1 + 0.055E^{0.1}Re_l^{0.16}\right)^{-1}$; $Re_l = Gd/\mu_l$; $Fr_l = G^2/\left(\rho_l^2 gd\right)$;

$If\ \ Fr_l \leq 0.05\ , EFr_l^{0.1-2Fr_l}\ instead\ of\ E\ and\ SFr_l^{0.5}\ instead\ of\ S$;

$F_M = \left\{1 + \frac{\Delta T_{bp}}{\Delta T_{id}}|y - x|^{c_1}(P/10^5)^{c_2}\left[1 + c_3 exp\left(-\frac{q}{3\times10^5}\right)\right]\right\}^{-1}$; c_1=-0.29; c_2=-0.9; c_3=-0.87

4.Sami et al. [27](1992)

$h_{tp,m} = 0.015\frac{\lambda_l}{d}\left(\frac{Gd}{\mu_l}\right)^{0.62} A\frac{\lambda_l^{0.3}}{100}$; $A = 1 - 0.79[|\tilde{y}_1 - \tilde{x}_1| + |\tilde{y}_2 - \tilde{x}_2|]^{0.82}$

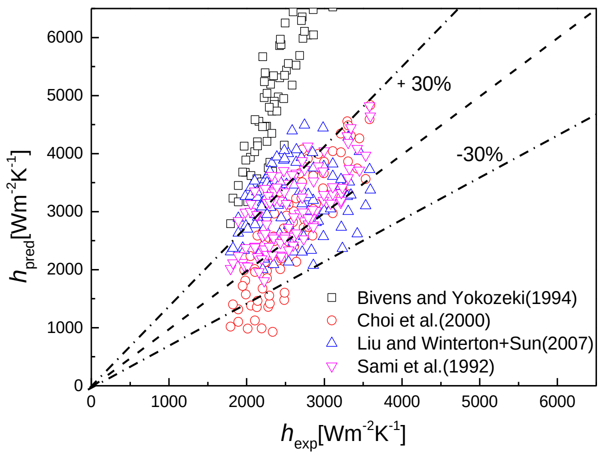

Fig.7. L-41b experimental data compared with correlation

Tab.5. Deviations between predicted and experimented flow boiling heat transfor coefficient

Saturation	Heat	Mass	Bivens and Yokozeki		Choi et al.		Liu and Winterton		Sami et al.	
Temp.(°C)	flux(kWm^{-2})	flux(kgm^{-2}s^{-1})	AAD	RMS	AAD	RMS	AAD	RMS	AAD	RMS
10±0.5	10	200	98.73	99.06	27.66	9.45	84.48	73.96	39.37	17.42
		300	107.13	117.56	30.02	10.98	72.83	57.88	42.34	19.97
		400	102.73	108.62	26.67	8.39	59.51	42.03	31.25	13.16
	5	200	106.27	121.71	15.15	3.90	32.26	13.02	10.71	1.34

		300	133.16	191.06	15.69	3.89	30.66	14.06	11.30	1.54
		400	149.75	246.73	16.02	4.81	30.05	14.60	10.24	1.53
20±0.5	10	300	112.87	133.39	23.07	6.40	29.74	13.55	26.97	8.90
		400	122.93	158.10	23.49	6.57	34.55	17.73	26.95	9.14
		500	125.31	164.72	21.94	6.09	37.76	20.65	26.83	8.59
	5	300	141.33	220.17	15.44	5.14	22.31	6.11	4.56	0.30
		400	161.11	285.18	15.41	5.59	28.45	10.46	2.79	0.11
		500	176.98	350.02	17.42	6.81	32.72	13.97	8.40	1.07

4.3 Development of a new correlation for L-41b in smooth tubes

Among the results, the correlation of Choi achieves the best agreement with experimental data, although, it underestimates the measured heat transfer coefficients in low quality of below 0.3. In the present study, a new correlation will be developed for L-41b in smooth tubes based on Choi et al. model. The heat transfer coefficient is calculated by combining the contributions of the nucleate boiling and forced convective mechanisms by a superposition model.

$$h_{tp} = Eh_{cv} + F_M S h_{nb} \tag{13}$$

Eh_{cv} is the contribution of the forced convective mechanism. E is the forced convective heat transfer enhancement factor and h_{cv} is calculated from Dittus-Boelter equation.

$$h_{sp} = 0.023(Re_l)^{0.8}(Pr_l)^{0.4}(\lambda_l/d) \tag{14}$$

$$E = C_1 Bo^{C_2} X_{tt}^{C_3} \tag{15}$$

h_{nb} is calculated from Cooper's pool boiling correlation. S is the suppression factor.

$$h_{nb} = 207(\lambda_l/D_{bl})[qD_{bl}/(\lambda_l T_{sat})]^{0.674}(\rho_v/\rho_l)^{0.581} Pr_l^{0.533} \tag{16}$$

$$S = C_4 Co^{C_5} \tag{17}$$

F_M is the mixture correction factor, which is used to model the mass transfer resistance effect. A correction for F_M is developed based on the experimental data obtained in this work. The values of C_1-C_5 and C_M in equation (19) are empirical constants and obtained by an iteration process to minimize the errors between the heat transfer coefficient calculated from the above correlations and experimental results. These values are represented in Tab.6. Empirical parameter F_M can be incorporated into correlation for mixtures.

$$F_M = \{1 + C_M[C_{p,l}(T_{dew} - T_{bp})/H_{lv}]\}^{-1} \tag{18}$$

$$h_{tp} = C_1 Bo^{C_2} X_{tt}{}^{C_3} h_{sp} + C_4 Co^{C_5}\left(1 + \frac{(T_{dew} - T_{bp})C_M}{h_{lv}}\right)^{-1} h_{nb} \tag{19}$$

Tab.6. Fitting model empirical constant

C_1	C_2	C_3	C_4	C_5	C_M
0.272	-0.139	-0.647	2.907×105	0.0244	9.704×105

Fig.8 presents the comparison of the predicted values of the new correlation with the experimental data. As shown in Fig.8, the deviations of the new correlation are within -24.98% to +14.68% from the experimental data and the 95% prediction values are within ±15%. Therefore, the new correlation can provide good predictions to the flow boiling heat transfer of L-41b inside the 8.0 O.D. horizontal smooth tubes.

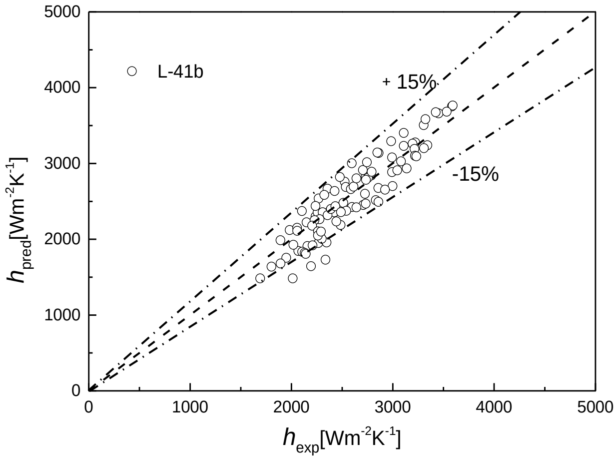

Fig.8. Experimental data compared with correlation

5 Conclusions

Flow boiling heat transfer characteristics for the binary mixtures of L-41b in a horizontal smooth tube were studied. The influences of saturation, heat flux and mass flux to the heat transfer characteristic were examined and discussed.

The experimental flow boiling heat transfer coefficients were compared with those calculated by the four typical correlations. The correlation of Choi achieves the best agreement with experimental data. The total absolute average deviation is 20.7%, and approximately 90% of experimental points are in an error bandwidth of ±30% of the prediction.

A modified correlation was developed based on the previous research (Choi et al.) and the experimental data in this study. The predicted values from the modified correlation show an acceptable agreement with the experimental data with a relative deviation within -24.98% to +14.68% and the 95% prediction values are within ±15%. Therefore, it can be used to predict the saturated flow boiling heat transfer coefficients of L-41b in horizontal smooth tube.

ACKNOWLEDGEMENT

This work was supported by Fujian Education Department Youth Education Technology Project (NO.JAT170388) and Scientific Research Foundation of Fujian University of Technology (NO.GY-Z160136)

References

[1] Adrian M.B., Joaquin N.E., Angel B, at el. Drop-in energy performance evaluation of R1234yf and R1234ze(E) in a vapor compression system as R134a replacements. *Appl. Therm. Eng.*, 71(2014) 259-265.

[2] Mark O.M., Andrei F.K., J. Steven Brown, et al. A thermodynamic analysis of refrigerants: Possibilities and tradeoffs for Low-GWP refrigerants. *Int. J. Refrig.*, 2014, 38, pp: 80-92.

[3] Bhatkar V W, Kriplani V M, Awari G K. Alternative refrigerants in vapour compression refrigeration cycle for sustainable environment: a review of recent research[J]. *Int. J. Environ.Sci. & Tech.*, 2013, 10, pp: 871-880.

[4] Bansal P., Vineyard E., Abdelaziz O. Advances in household appliances−A review. *Appl. Therm. Eng.*, 2011, 31, pp: 3748-3760.

[5] Calm J.M. The next generation of refrigerants historical review consideration and outlook. *Int. J. Refrig.*, 2008, 31, pp: 1123-1133.

[6] Mota-Babiloni A, Navarro-Esbrí J, Makhnatch P, et al. Refrigerant R32 as lower GWP working fluid in residential air conditioning systems in Europe and the USA[J]. *Renewable & Sustainable Energy Reviews*, 2017, 80, pp: 1031-1042.

[7] Zilio C, Brignoli R, Kaemmer N, et al. Energy efficiency of a reversible refrigeration unit using R410A or R32[J]. *Hvac & R Research*, 2015, 21, pp: 502-514.

[8] Mota-Babiloni A, Navarro-Esbrí J, Molés F, et al. A review of refrigerant R1234ze(E) recent investigations[J]. *Appl. Therm. Eng.*, 2016, 95, pp: 211-222.

[9] Wang X, Amrane K. AHRI Low Global Warming Potential Alternative Refrigerants Evaluation Program (Low-GWP AREP)–Summary of Phase I Testing Results[J]. *Journal of the Taiwan Institute of Chemical Engineers*, 2014, 45, pp: 996-1000.

[10] Xudong Wang, Karim Amrane. AHRI Low Global Warming Potential Alternative Refrigerants Evaluation Program (Low-GWP AREP)-Summary of Phase I Testing Results. *15th International Refrigeration and Air Conditioning Conference at Purdue*, USA: Purdue University e-Pubs, 2014

[11] Akasaka R. Thermodynamic property models for the difluoromethane (R-32) + trans-1,3,3,3-tetra-fluoropropene (R-1234ze(E)) and difluoromethane +2,3,3,3-tetrafluoropropene (R-1234yf) mixtures. *Fluid Phase Equilib.*, 2013, 35, pp: 98-104.

[12] Cui J, Bi S, Meng X, et al. Surface Tension and Liquid Viscosity of R32+R1234yf and R32+R1234ze[J]. J. Chem. & Eng. Data, 2016, 61, pp: 950-957.

[13] Jia T, Bi S, Hu X, et al. Volumetric properties of binary mixtures of {difluoromethane (R32) + trans-1,3,3,3-tetrafluoropropene (R1234ze(E)) at temperatures from 283.15 K to 363.15 K and pressures up to 100 MPa[J]. *J. Chem. Thermodynamics*, 2016, 101, pp: 54-63.

[14] Cheng Z, Wang B, Shi W, et al. Numerical Research on R32/R1234ze(E) Air Source Heat Pump under Variable Mass Concentration[J]. *Int. J. Refrig.*, 2017, 82, pp: 1-10.

[15] Lee H, Troch S, Hwang Y, et al. LCCP evaluation on various vapor compression cycle options and low GWP refrigerants[J]. *Int. J. Refrig.*, 2016, 70, pp: 128-137.

[16] Francisco Moles，Joaquin Navarro-Esbri，Bernardo Peris，et al. Theoretical energy performance evaluation of different single stage vapour compression refrigeration configurations using R1234yf and R1234ze(E) as working fluids. *Int. J. Refrig.*, 2014, 44, pp: 141-150.

[17] Adrian M.B.， Joaquin N.E.， Angel B.， et al. Theoretical comparison of low GWP alternatives for different refrigeration configurations taking R404A as baseline. *Int. J. Refrig.*， 2014, 44, pp: 81-90.

[18] Adrian M.B., Joaquin N.E., Angel B., at el. Drop-in energy performance evaluation of R1234yf and R1234ze(E) in a vapor compression system as R134a replacements. Appl. Therm. Eng., 2014, 71, pp: 259-265.

[19] In S, Cho K, Lim B, et al. Performance test of residential heat pump after partial optimization using low GWP refrigerants[J]. *Appl. Therm. Eng.*, 2014, 72, pp: 315-322.

[20] Hossain M. A., Onaka Y., Hasan M. M. Afron, et al. Heat transfer during evaporateon of R1234ze(E), R32, R410A and a mixture of R1234ze(E) and R32 inside a horizontal smooth tube. *Int. J. Refrig.*, 2013, 36, pp: 465-477.

[21] D.L. Bivens, A. Yokozeki. Heat transfer coefficients and transport properties for alternative refrigerants. *In: Proceeding of International Refrigeration Conference at Purdue*, IN, USA. 1994, pp: 299-304.

[22] Choi T.Y., Kim Y.J., Kim, M.S., et al. Evaporation heat transfer of R-32, R-134a, R-32/R-134a, and R-32/125/134a inside a horizontal smooth tube. Int. J. Heat & Mass Trans., 2000, 43, pp: 3651-360.

[23] Liu Z., Winterton R.H.S. A general correlation for saturated and subcooled flow boiling in tubes and annuli, based on a nucleate pool boiling equation. *Int. J. Heat Mass Trans.*, 1991, 34, pp: 2759-2766.

[24] Sun Z, Gong M, Li Z, et al. Nucleate pool boiling heat transfer coefficients of pure HFC134a, HC290, HC600a and their binary and ternary mixtures[J]. *Int. J. Heat & Mass Trans.*, 2007, 50, pp: 94-104.

[25] S.M. Sami, J. Schnotale., J.G. Smale. Prediction of the heat transfer characteristics of R22/R152a/R114 and R22/R152a/R124. *ASHRAE Trans.*, 1992, 98, pp: 51-58.

[26] Qiu J, Zhang H, Yu X, et al. Experimental investigation of flow boiling heat transfer and pressure drops characteristic of R1234ze(E), R600a, and a mixture of R1234ze(E)/R32 in a horizontal smooth tube[J]. *Advances in Mechanical Engineering*, 2015, 7, pp: 1-12.

[27] Kedzierski, A., Kim, J.H., Didion, D.A. Cause of the apparent heat transfer degradation for refrigerant mixtures. *ASME HTD Two-Phase Flow and Heat Trans.*, 1992, 197, pp: 149-158.

[28] Moffat, R.J. Describing the uncertainties in experimental results. *Exp. Therm. Fluid*, 1988, 1, pp: 3-17.

Nomenclature

AAD	absolute average deviation, $[(1/n)\Sigma(\mid h_{cal}-h_{exp}\mid/h_{exp})]\times100\%$		*Greek letter*
Bo	Boiling number $[Bo=q/(Gh_{fg})]$	μ	viscosity, Pas
*C*p	isobaric specific heat, $J\cdot kg^{-1}\cdot K^{-1}$	ε	void fraction
Co	convection number $[\{(1-x)/x\}^{0.8}(\rho_l/\rho_v)^{0.5}]$	Φ	two-phase flow multiplier
d	tube diameter, m	λ	thermal conductivity, $W\cdot m^{-1}K^{-1}$
h	heat transfer coefficient, $kW\cdot m^{-2}\cdot K^{-1}$	σ	surface tension, $N\cdot m^{-1}$
E	enhancement factor	ρ	density, $kg\cdot m^{-3}$
Fr	Froude number $[G^2/(\rho^2 gd)]$	v	kinematic viscosity, $m^2\cdot s^{-1}$
g	acceleration of gravity, $m\cdot s^{-2}$		
G	mass flux, $kg\cdot m^{-2}\cdot s^{-1}$		*Subscripts*
H_{lv}	latent heat of vaporization, $J\cdot kg^{-1}$	ave	average
m_{total}	total mass velocity of liquid plus papor	cal	calculation
M	molecular weight	cv	convection
P	pressure, kPa	exp	experimental
Δp	pressure drop, Pa	in	inner
dp/dz	frictional pressure gradient(Pam^{-1})	l	liquid
Pr	Prandtl number	lo	liquid only
q	heat flux, $kW\cdot m^{-2}$	lv	liquid-vapor
Q	heat transfer rate of the whole test section, $J\cdot s^{-1}$	mix	mixture
Re	Reynolds number	nb	nucleate boiling
RMS	root mean square deviation, $[(1/n)\Sigma(\mid h_{cal}-h_{exp}\mid/h_{exp})^2]\times100\%$	out	outer
S	suppression factor	pb	nucleate boiling
T	temperature, K or ℃	pred	predicted
ΔT	temperature glide, K or ℃	preh	preheater
We	Weber number $[G^2d/(\rho\sigma)]$	sat	saturation